



Fluorescence-guided minimally-invasive surgery for colorectal liver metastases, a systematic review

Okker D. Bijlstra^{1,2}, Friso B. Achterberg¹, Lodi Grosheide², Alexander L. Vahrmeijer¹, Rutger-Jan Swijnenburg²

¹Department of Surgery, Leiden University Medical Center, Leiden, The Netherlands; ²Department of Surgery, Cancer Center Amsterdam, Amsterdam UMC, University of Amsterdam, Amsterdam, The Netherlands

Contributions: (I) Conception and design: OD Bijlstra, FB Achterberg, RJ Swijnenburg; (II) Administrative support: None; (III) Provision of study materials or patients: None; (IV) Collection and assembly of data: OD Bijlstra, FB Achterberg, L Grosheide; (V) Data analysis and interpretation: OD Bijlstra, L Grosheide; (VI) Manuscript writing: All authors; (VII) Final approval of manuscript: All authors.

Correspondence to: Rutger-Jan Swijnenburg, MD, PhD. Department of Surgery, Cancer Center Amsterdam, Amsterdam UMC, University of Amsterdam, Meibergdreef 9, 1105 AZ Amsterdam, The Netherlands. Email: r.j.swijnenburg@amsterdamumc.nl.

Abstract: Approximately 25–30% of patients with colorectal cancer (CRC) develop liver metastases (CRLM) over the course of the disease. To achieve curative surgical treatment of liver metastases is still considered as the gold standard. A shift from open to laparoscopic and robot-assisted surgery has occurred over the past decades. Extensive research has been performed using both preoperative as well as intraoperative imaging techniques to improve treatment planning, intraoperative tumor detection and evaluation of resection margins. Recently, increasing interest in near-infrared fluorescence (NIRF) imaging emerged as an intraoperative imaging modality in liver surgery. NIRF-guided liver surgery with the fluorescent dye indocyanine green (ICG) has been implemented as standard-of-care in various centers across the globe to aid in lesion differentiation and guidance of surgical margins. However, the low specificity and high false-positive rates of ICG in intraoperatively found lesions have led to the demand and development of tumor-specific fluorescent probes and improved camera systems. Here, we present a systematic review of available literature on intraoperative fluorescence imaging for minimally invasive CRLM surgery. Furthermore, we emphasize on fluorescent enhancement patterns, recent developments and future perspectives concerning fluorescent dyes and imaging techniques to optimize clinical application.

Keywords: Colorectal liver metastases (CRLM); near-infrared fluorescence imaging (NIRF imaging); minimally-invasive hepatic surgery; molecular imaging

Received: 13 July 2020; Accepted: 31 December 2020; Published: 25 July 2021.

doi: 10.21037/ls-20-108

View this article at: <http://dx.doi.org/10.21037/ls-20-108>

Introduction

Colorectal cancer (CRC) is the third most common malignancy worldwide, and the second most lethal one, with the highest incidence rates in Europe and Australia (1). Secondary prevention measures in several western countries, such as population screening, has resulted in an initial increased incidence of CRC, and closer monitoring. Approximately 25–30% of patients diagnosed with CRC either have synchronous or develop metachronous colorectal liver metastases (CRLM) (1-3). To this day, surgery remains the preferred curative

treatment option for CRLM, with 5-year-survival rates ranging from 32–56% (2). Eligibility for resection of CRLM is determined by a multidisciplinary tumor board after four phase computed tomography (CT) in most countries. Some centers also perform magnetic resonance imaging (MRI) and/or positron emission tomography computed tomography (PET-CT). Since the abovementioned imaging modalities all have their benefits and limitations, a combination of imaging strategies has become standard practice for tumor detection, staging and treatment planning and postoperative treatment evaluation.

When considered suitable for resection, either open or minimally invasive surgery is performed, with or without radiofrequency ablation (RFA) or microwave ablation (MWA). To assist the surgeon in the hepatic resection(s), intraoperative ultrasonography (IOUS) is routinely performed, either by the radiologist or surgeon. IOUS provides the surgeon with the most up-to-date information on number and size of CRLM, and its relation to anatomical structures (e.g., vascular structures and the biliary tract). IOUS may identify additional lesions in up to 33% of patients undergoing hepatic resection compared to preoperative CT imaging (4). However, superficial and subcapsular lesions may easily be missed on IOUS, as well as lesions smaller than 3 mm (5,6). Furthermore, those lesions are also hard to identify with the naked eye. A shift from open liver surgery to laparoscopic and robot-assisted liver surgery has occurred in the past decade, and is expected to continue (7,8). IOUS is especially technically challenging in minimally invasive procedures given its limitations in free-range of motion. In open surgery, surgeons may also use tactile information as a diagnostic method and to evaluate tumor margins during parenchymal resections. However, palpation has low diagnostic value and is very limited in laparoscopic and robot-assisted surgery, since no haptic feedback is provided by the surgical console and tactile feedback is extremely limited in regular laparoscopic surgery.

Both minimally invasive techniques resulted in decreased complications, shorter hospital stay, and comparable oncological outcomes compared to open surgery (9,10). This shift combined with the limitations of IOUS and palpation have resulted in the increased interest in other intraoperative imaging modalities such as near-infrared fluorescence (NIRF) imaging (11-13). Since tactile information lacks in minimal invasive surgery, and small capsular and subcapsular lesions are easily missed by IOUS, NIRF imaging has even more potential benefits in these procedures. Furthermore, during minimally invasive procedures, NIRF imaging can be projected onto the regular laparoscopic video feed, creating a fluorescence-overlay. This can be switched on and off according to the surgeon's preference.

Extensive research in NIRF-guided surgery has been performed in the past decade, resulting in over 1,500 published articles (PubMed) from 01-01-2008 until 30-04-2020, and 730 publications specifically for hepatic surgery. NIRF surgery has proven to be an effective imaging technique in liver surgery (14). NIRF imaging is superior to US, CT and MRI in terms of spatial and temporal

resolution. Moreover, NIRF does not produce ionizing radiation, making it safe for both the clinician and the patient (15,16). Indocyanine green (ICG) is the most widely used and studied fluorescent dye. Most surgical camera systems are optimized for the wavelength to excite and detect ICG (excitation wavelength: 780 nm, emission wavelength: 805 nm) (17). This resulted in numerous clinically approved, ISO certified imaging systems able to produce NIRF overlay images during both open and minimally invasive surgery, providing the surgeon with real-time feedback.

In this paper, we have reviewed studies on the clinical applications, recent developments and future perspectives on NIRF-guided surgery in CRLM. Furthermore, we will elaborate on the physiology of ICG, and optimal dose and timing of currently used fluorescent dyes. Finally, different fluorescent enhancement patterns which may be present during fluorescence-guided resection of liver lesions will be discussed. We present the following article in accordance with the PRISMA reporting checklist (available at <http://dx.doi.org/10.21037/ls-20-108>).

Literature search

The PubMed database was searched by the scientific librarian of the Leiden University Medical Center. Keywords of the search strategy consisted of “near-infrared fluorescence” AND “liver tumor(s)”. Inclusion criteria were: (I) use of intraoperative NIRF; (II) liver resection planned and/or performed; (III) human studies only; and (IV) English manuscripts only. Exclusion criteria were: (I) other malignancy than CRLM; (II) review articles; (III) less than five patients, and (IV) no full text available. Outcomes of interest were sensitivity, dose and timing of fluorescent dye injection and R0 and R1 resection rates.

Results

A total of 495 studies, published between 01-01-2005 and 30-06-2020, were initially included. After removing studies where no full text was available, studies without human study subjects and studies that were not written in English, a total 249 studies were screened for eligibility on title and abstract. Screening by title and abstract excluded another 229 articles, mainly because studies were either not conducted on humans or focused on malignancies other than CRLM. Twenty full manuscripts were read, after which nine studies focusing on other malignancies were excluded. *Figure 1* summarizes the selection of studies

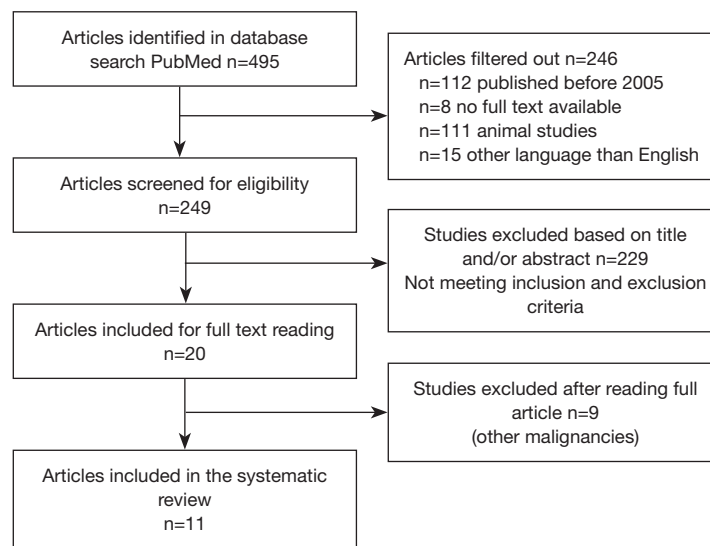


Figure 1 Summary of study selection.

showcased in a flowchart.

Basic properties of fluorescence imaging

The quantum yield of fluorescence depends on complex concepts of scattering, reflection, transmission and absorption of the emission and excitation light of the tissue molecules. Fluorescent imaging requires a light source sending out photons at a specific wavelength to excite an exogenous contrast agent, or fluorophore (e.g., ICG). Specifically to surgical use, these photons have to travel through tissue to reach the fluorophore in the target organ or lesion. Upon entering and passing through tissue, photons are either absorbed, reflected or refracted. When the photon enters the target tissue, absorption by a fluorophore leads to a gain of energy of the fluorophore which then enters the excited state for 10^{-8} seconds. After returning to the ground state the photon is emitted. The change in energy between the excitation photon and the emitted photon results in a wavelength change, known as the Stokes shift (18). The emitted photons are also influenced by reflection and refraction when traveling through different types of tissue again, resulting in scattering. This makes interpretation and quantification of NIRF images complex (19).

Physiology of ICG

ICG, the most frequently used fluorescent dye in hepatic

surgery, is an amphiphilic molecule able to bind to either hydrophilic or lipophilic molecules. ICG transfers actively from the plasma into hepatic parenchymal cells, and is excreted exclusively via the biliary system (20). Polymers (aggregates) have weaker fluorescence yield than free ICG monomers or ICG bound to plasma proteins (20). Protein-bound ICG emits light that peaks at approximately 832 nm when illuminated with near-infrared light (750–810 nm) (21). Water is the preferred solvent for intravenous injection of ICG for optimal fluorescent intensity, as saline promotes aggregation (17).

The fluorescence properties of ICG were already revealed in detail in the 1970s (22), and real-time fluorescence imaging using ICG began, with clinical application in the early 1990s in the field of ophthalmology for fundus angiography. In the twenty-first century, the application of ICG fluorescence imaging was extended to surgery as an intraoperative navigation tool for lymphatic flow, sentinel lymph nodes, blood flow during coronary artery bypass grafting and clipping of cerebral aneurysms. For assessment of liver function the ICG retention test (ICG R15) is a well-known function parameter. Clearance of ICG is impaired when >15% of the dye remains in the plasma 15 minutes after injection of 0.5 mg/kg ICG (23). Interestingly, little attention had been paid to the fluorescence properties of ICG in the fields of hepatic surgery until Japanese groups started with intraoperative fluorescence cholangiography focusing on another properties of ICG (i.e., biliary excretion). During liver surgery a specific enhancement

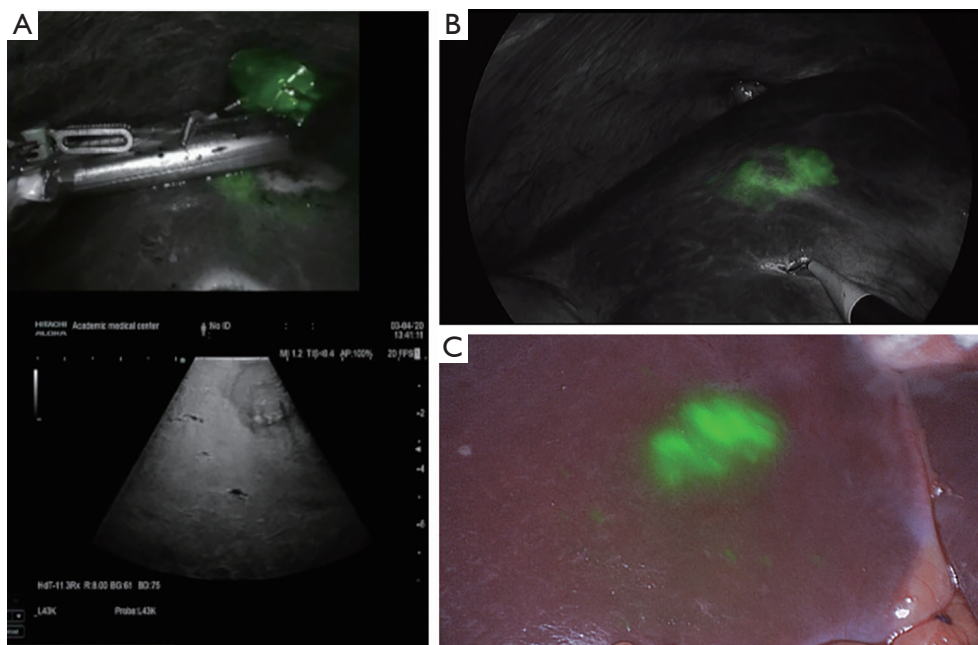


Figure 2 Two images of fluorescent enhancement patterns surrounding CRLM. (A) Typical rim-shaped enhancement pattern of capsular CRLM with simultaneous IOUS guidance; (B) rim-shaped fluorescent enhancement pattern surrounding a capsular CRLM; (C) circular-shaped enhancement pattern of subcapsular CRLM. CRLM, colorectal liver metastasis; IOUS, intraoperative ultrasonography.

pattern of fluorescent light was observed after preoperative ICG injection in patients with hepatocellular carcinoma (HCC) (24). This discovery led to an increase in studies for the application of ICG in liver surgery.

Fluorescence imaging during CRLM surgery

Clinical applications

The typical enhancement pattern of ICG in CRLM after a single 24-hour preoperative IV-dose is a rim-shaped pattern (Figure 2A,B). ICG accumulates in the tumor periphery, which is unable to excrete ICG in the bile due to immature hepatocytes (25). In contrast, normal liver parenchyma excretes ICG into the biliary tract within 30 minutes to 2 hours after injection; resulting in the typical enhancement pattern. However, care must be taken regarding the enhancement pattern, since the maximum penetration depth of fluorescent light is approximately 5–8 mm in liver tissue (26). One must imagine the fluorescent rim as a three-dimensional layer surrounding the complete tumor. A capsular hepatic metastasis shows the typical enhancement pattern, whereas subcapsular lesions may become visible as a circular shaped spot (Figure 2C). Consequently, lesions

located more centrally in the liver (deeper than 8 mm below the capsula) are not directly visualized by NIRF imaging. However, these lesions are also surrounded by ICG. Therefore, NIRF imaging can also be used for assessment of the resection margins deeper in the liver parenchyma, for example during segmental or hemi-hepatectomies. An overview of studies focusing on intraoperative NIRF imaging of CRLM is displayed in Table 1.

Dose and timing

Essential in the use of NIRF-guided surgery is optimal dose and timing in order to obtain adequate contrast between the tumor and surrounding tissue; the signal-to-background ratio (SBR). Studies focusing on translating new fluorescent dyes always aim to establish information on safety and efficacy and the ideal dose and time of injection of the dye for optimal SBRs (27). The SBR of NIRF imaging with ICG is usually high (>5), mainly as a result of the optimization of imaging systems for ICG. SBRs of tumor-specific imaging probes are usually lower, ranging from 1.5–3.5 (28).

However, for CRLM, optimal dose and timing of ICG have not yet been standardized (29). Most studies used the

Table 1 An overview of available literature on the use of near-infrared fluorescent imaging with ICG in surgical treatment of CRLM

Author	Year	Country	Design	#Patients [lesions]	Fluorescent dye	Dose & timing	TP (%), FP (%)	Sensitivity (%), PPV (%)	#Additional lesions (%TP)	R0 (%), R1 (%)
Ishizawa <i>et al.</i>	2009	Japan	Prospective cohort	12 [28]	ICG	0.5 mg/kg, 1–14 days	100, 0	100, 100	0	NR
Uchiyama <i>et al.</i>	2010	Japan	Prospective cohort	32 [56]	ICG	0.5 mg/kg, 14 days	93.1, 6.9	98.1*, 96.3*	4 (50.0)	NR
Peloso <i>et al.</i>	2013	Italy	Prospective cohort	25 [78]	ICG	0.5 mg/kg, 24 hours	98.7, 1.3	NR	23 (95.7)	98.7, 1.3
van der Vorst <i>et al.</i>	2013	Netherlands	Prospective cohort	40 [97]	ICG	10 or 20 mg, 24/48 hours	100, 0	73 [§] , NR	5 (100.0)	NR
Kudo <i>et al.</i>	2014	Japan	Prospective cohort	6 [16]	ICG	0.5 mg/kg, 1–14 days	NR	69, NR	NR	NR
Abo <i>et al.</i>	2015	Japan	Prospective cohort	36 [36]	ICG	0.5 mg/kg, 4–7 days	NR	86, NR	NR	NR
Kaibori <i>et al.</i>	2016	Japan	Prospective cohort	13 [NR]	ICG	0.5 mg/kg, 1–14 days	NR	96, NR	4 (100.0)	NR
Terasawa <i>et al.</i>	2017	Japan	Prospective cohort	NR [42]	ICG	0.5 mg/kg, 1–3 days	NR	85, NR	4 (100.0)	NR
Handgraaf <i>et al.</i>	2017	Netherlands	Retrospective cohort	86 [106]	ICG	10 or 20 mg, 24/48 hours	NR	83 [§] , NR	NR	83, 17
Boogerd <i>et al.</i>	2017	Netherlands	Prospective cohort	12 [18]	ICG	10 mg, 24 hours	NR	92, 75	3 (100.0)	88, 12
Lieto <i>et al.</i>	2018	Italy	Prospective cohort	6 [8]	ICG	0.5 mg/kg, 24 hours	100, 0	100, NR	1 (100.0)	NR

*, Combined sensitivity for IOUS and NIRF imaging; [§], 100% of superficial lesions. ICG, indocyanine green; CRLM, colorectal liver metastases; TP, true positive; FP, false positive; PPV, positive predictive value; R0, clear resection margin (≥ 1 mm); R1, positive resection margin (< 1 mm); NR, not reported; IOUS, intraoperative ultrasonography; NIRF, near-infrared fluorescence.

same dose of ICG (0.5 mg/kg) 1–14 days prior to surgery as in the ICG R15 test (30). van der Vorst *et al.* (25) compared four dose-timing intervals: two groups received a dose of 10 mg 24 and 48 hours prior to surgery, respectively. The other two groups were injected with 20 mg either 24 or 48 hours prior to surgery. No statistical difference was observed in the SBR in different groups. In most Asian studies however, a dose of 0.5 mg/kg is most frequently used. Recent preliminary results of a study in Italy concluded a dose of 0.2 mg/kg 24–48 hours prior to surgery was optimal when the ICG retention test was performed more than 7 days prior to hepatectomy. However, no correction for cirrhosis and ICG R15 was performed (31).

Patients initially considered to have unresectable disease at time of diagnosis of CRLM may receive neoadjuvant chemotherapy prior to surgery in order to reduce the amount and size of CRLM. In the United States of America

all patients with CRLM are treated with chemotherapy prior to surgery (32). This hepatotoxic systemic neoadjuvant chemotherapy may result in impaired liver function due to chemotherapy-associated liver injury (33). Krieger *et al.* (34) reported that ICG retention rates at 15 minutes of patients after receiving chemotherapy was significantly higher compared to the non-chemotherapy group. van der Vorst *et al.* (25) report that neoadjuvant chemotherapy has no significant influence on SBR using their 24 hours prior to surgery injection. Currently, there is no consensus on whether patients pretreated with chemotherapy should receive a different dose at a different time point.

Applications of ICG fluorescence imaging during liver surgery

First, NIRF-guided surgery is currently used for

Table 2 An overview of malignant and benign hepatic lesions and their appearance with WLI and fluorescent enhancement patterns

Lesion type	Appearance WLI	Fluorescent enhancement pattern
Malignant		
CRLM	Hard, pale tumor	Rim-shaped Negative contrast
HCC	Soft, pale tumor hemorrhage, necrosis and cirrhosis are common	
Well-differentiated		Rim-shaped
Poorly differentiated		Tumorous
CCA	Large, firm, white-gray tumor	Rim-shaped
Benign		
Von Meyenburg (bile duct proliferation)	Single or multiple subcapsular well circumscribed gray-white nodule	Small, well circumscribed lesion with ICG accumulation inside lesion
Hemangioma	Solitary 2–4 cm, soft red lesion	ICG accumulates around the lesion, blurry borders
Focal steatosis	Yellow, greasy and soft	Variable size and shape, usually blurry borders
Regenerative nodule	Well circumscribed circular lesion	Small, rim-shaped or well circumscribed ICG accumulation

WLI, white light imaging; CRLM, colorectal liver metastasis; HCC, hepatocellular carcinoma; CCA, cholangiocarcinoma; ICG, indocyanine green.

identification of liver lesions. Studies show sensitivities ranging from 73–100% for the intraoperative detection of CRLM (25,26,35–42). In a study consisting of 40 patients selected for NIRF-guided liver resections, 12% of subjects had additional metastases based on NIRF-imaging alone, compared to IOUS (25). In a retrospective multi-center analysis in 2017, significantly more additional metastases were identified in patients where NIRF imaging was performed compared to identification by inspection, palpation and IOUS (25% *vs.* 13%) (14). The additional lesions were mainly small lesions (mean size 3.2 mm) located at or right below the liver's surface, in a region where IOUS has low sensitivity. A negative contrast technique can also be used for lesions identification. With this approach, ICG is administered during the surgical procedure leading to fluorescent enhancement of the entire liver except for the CRLM (43).

Since ICG is a non-specific fluorescent dye, one of the potential drawbacks of NIRF-guided surgery for detection of additional lesion in patients with CRLM is a high false-positive rate ranging from 2–20% in the literature (25,37,44,45). False-positive rates are higher in patients with impaired liver function, especially with a shorter administration-to-surgery interval. Focal steatosis, cysts, hemangiomas,

regenerative nodules and bile duct proliferations have been reported as false-positives (*Figure 3A,B,C,D*). An overview of histopathological findings of the abovementioned benign lesions is shown in *Table 2*.

Second, prediction of surgical margin after resection could be performed real-time using NIRF imaging, without delay of sending a frozen section specimen to a pathologist. Currently, 14–28% of liver resections are considered as an R1 resection, leading to decreased survival (46–48). In some cases, achieving an oncological complete resection with a 1 mm margin is not technically possible. However, in other cases a tumor-negative resection seems feasible and these patients might potentially benefit from NIRF with ICG. Studies have been published on the positive staining technique using the presence of NIRF signal in the resection specimen or liver parenchyma as an indication for a tumor-positive margin. However, these studies are mainly proof-of-concept studies with relatively low inclusion numbers. Aoki *et al.* (49) compared R0-resections in CRLM in 12 patients receiving ICG to 40 patients without ICG in a non-randomized setting. In the NIRF-guided resection group all resections were radical, compared to 95% in the conventional imaging group. Currently, a multicenter trial, focusing on minimally invasive liver resections, initiated in

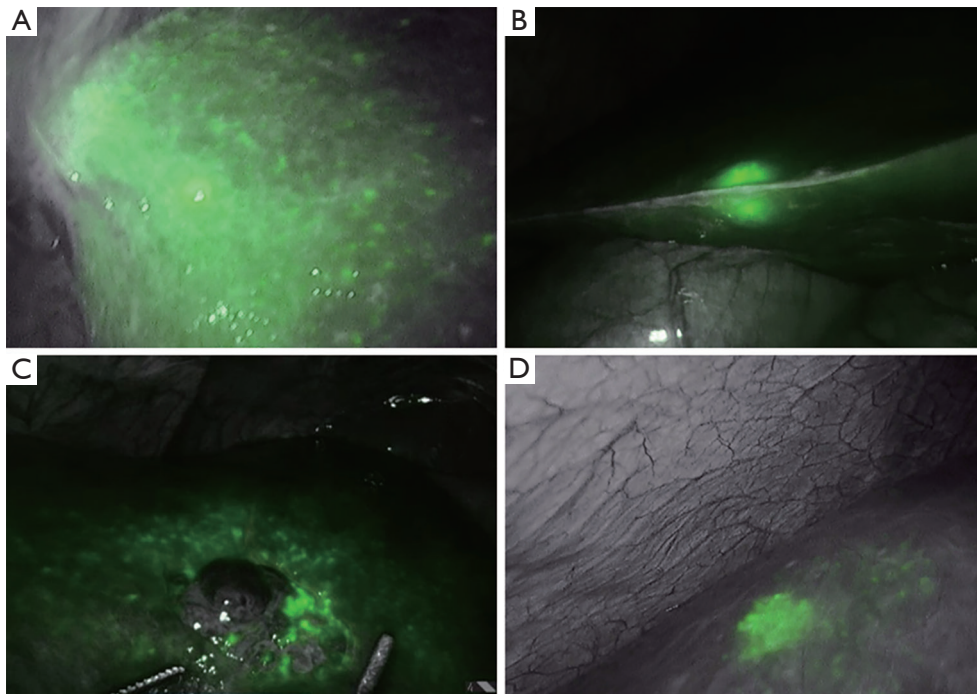


Figure 3 Images of fluorescent enhancement patterns described in and surrounding benign liver parenchyma. (A) Focal steatosis showing diffuse fluorescent enhancement; (B) a regenerative nodule showing a circular-shaped fluorescent enhancement pattern; (C) hemangioma showing a rim-shaped fluorescent enhancement; (D) von Meyenburg complex showing fluorescent enhancement.

our center is studying R1 resections in NIRF-guided liver metastasectomy.

Third, since ICG is cleared via the biliary tract, NIRF can be used for bile duct imaging. Intraoperative visualization of the biliary tract can aid the surgeon during left or right hemi-hepatectomy, for detection of bile duct injuries and for the evaluation of extrahepatic bile duct anatomy. Intravenous administration of 2.5 mg of ICG at least 15 minutes prior to imaging is the most common approach for fluorescence cholangiography (44,50,51). No clinical data is available on the visualization of bile duct injury with ICG. However, in patients with increased risk of bile duct injury NIRF imaging, compared to white light alone, can decrease the risk of injury (52,53).

Finally, selective liver segment staining can be used for segment resections. Either a negative or a positive contrast approach can be used. Negative contrast or the negative staining technique could be used for segment resection or hemi-hepatectomy. With this technique the liver remnant is stained whereas the part of the liver planned for resection lacks fluorescent enhancement (54).

A novel positive contrast technique for selective

segmental staining has recently been described by Ueno *et al.* (55) ICG dissolved in an embolic solution was injected in the desired segmental artery, followed by embolization of the branch. With this technique only the desired segment will show fluorescent enhancement, guiding the surgeon in segment resection.

Recent developments and future perspectives

Recent developments of NIRF-guided liver surgery mainly aim to establish the clinical relevance of the technique. In this perspective, the MIMIC-trial, a prospective multicenter registration study is being performed by our study group (Dutch Trial Registry: NL7674). The MIMIC-trial aims to investigate whether the use of NIRF-imaging during minimally invasive resection of CRLM can predict the tumor-margin *in vivo* which may lead to higher radical resection rates. Consecutively, long-term disease-free survival and overall survival will be studied.

Although NIRF camera systems for open surgery are able to display an overlay image, the nature of the procedure will still force a clinician to use a screen outside the surgical

field. To this day, the surgeon has to switch views from the patient on the operation table to a screen and vice versa. Therefore, new tools (e.g., by means of augmented reality) are being designed to create a true real-time fluorescent overlay over the operation bed (56).

Real-time overlay

In laparoscopic and robot-assisted (liver) surgery, a real-time fluorescent overlay can be projected over the operation field and displayed on the operation screen(s). In open liver surgery this is not yet possible. Therefore, new technological advancements are required for optimal integration of fluorescence in open liver surgery. One of the possibilities for the implementation is a real-time augmented reality fluorescent overlay with the HoloLens 2. HoloLens offers a mixed reality experience by presenting holograms in the field of view of the surgeon. As a result, the surgeon is able to visualize the surgical field and the fluorescent overlay at the same time.

Back-table pathology

Besides direct intraoperative applications, NIRF-imaging is often used for real-time back-table pathology assessment of resection margins. The resected liver specimen will be analyzed directly after resection in a closed-field fluorescent camera and mapped for fluorescence patterns. In order to become a reliable evaluation method of resection margins the behavior of the particular fluorescent dye and its histopathological characteristics should be thoroughly understood and fluorescence patterns should be translational to pathology findings.

A recent study performed at Stanford University described real-time back-table specimen mapping of resected head and neck cancer specimen to detect closest tumor-to-margins areas for surgical margin prediction (57). A comparable strategy is currently being studied for CRLM.

Tumor-specific imaging probes

One of the drawbacks of NIRF imaging with ICG is the low specificity of the dye leading to false-positive results. Tumor-specific imaging using a binding moiety (e.g., antibodies) can help to reduce false-positive rates. Carcinoembryonic antigen is overexpressed in over 90% of colorectal adenocarcinomas (58). SGM-101 (anti-CEA antibody labeled to a fluorescent dye) showed promising

results in NIRF-guided CRC surgery (27,59,60). Recently, SGM-101 has been studied by our group as tumor-specific fluorescence imaging probe for CRLM. All 12 liver metastases from colorectal origin were identified by NIRF imaging with SGM-101. Two false positive lesions were reported (61). The authors conclude SGM-101 is a promising alternative or adjunct to ICG. A larger trial should be conducted to study the added value of SGM-101 compared to ICG. This probe may be especially useful in patients with their primary tumor still *in situ*, with lymph node metastases or peritoneal metastases as these lesions all express carcinoembryonic antigen. Furthermore, since more tumors express CEA (e.g., pancreatic ductal adenocarcinoma) this probe can be applied for tumor detection and resection margin assessment of various tumors and its metastases (27). For CRLM, or CRC in general, more valuable targets for imaging have been investigated, creating possibilities for CEA negative tumors.

NIR-II window

The second near-infrared wavelength window (NIR-II) ranges from 1,000–1,700 nm and enables contrast enhanced fluorescence imaging tissue at depths of several millimeters. The longer wavelengths utilized in the NIR-II window enable deeper tissue penetration than NIR-I imaging because of reduced photon absorption and scattering (62). First-in-patient results of NIR-II imaging are documented in a recently published article by Hu *et al.* (63). The authors included 23 patients with primary or metastatic liver tumors imaged in both the NIR-I and NIR-II window, and found higher sensitivity in tumor detection (90.6% *vs.* 100%), and higher SBR (1.45 *vs.* 5.33) in the NIR-II window. Another benefit from NIR-II imaging is the reduced influence from surrounding light. The authors have conducted all their experiments while surrounding operating lights were switched on, and reported no influence on the imaging data. However, several limitations need to be overcome before the clinical implementation of NIR-II fluorescence imaging. First, current problems regarding inorganic fluorophores are non-specific tissue targeting, slow metabolism and high toxicity (64). Second, organic NIR-II fluorophores lack fluorescence performance due to solvent interaction in the plasma *in vivo* (65). Third, various molecular interactions lead to a decreased intensity of emitted light from fluorescent molecules, i.e., quenching (65–67). Finally, current NIR-II fluorescent molecules are hydrophobic and have poor physiological stability (64).

Conclusions

NIRF-imaging is being used in a growing number of hospitals for intraoperative detection and surgical guidance during minimally invasive resections of CRLM. Moreover, many studies are being conducted regarding the exact behavior of ICG. Thus far, the use of ICG during liver surgery is generally experience-based. For optimal and global implementation of NIR imaging with ICG ideal dose and timing guidelines still have to be developed. This requires larger patient series studying clinical benefit.

Furthermore, there is growing interest in new, tumor-specific, fluorescent probes for more accurate tumor detection, resection margin evaluation and lower false-positive rates leading to more parenchymal preserving surgery. Finally, research in the NIR-II spectrum is only at its starting point but may become an important emerging imaging strategy.

Acknowledgments

Walaeus Library Leiden for performing the literature search.

Funding: None.

Footnote

Provenance and Peer Review: This article was commissioned by the Guest Editors (Hendrik A. Marsman and Mark C. Boonstra) for the series “Clinical Applications of Fluorescence Imaging in Laparoscopic Surgery” published in *Laparoscopic Surgery*. The article has undergone external peer review.

Reporting Checklist: The authors have completed the PRISMA reporting checklist. Available at <http://dx.doi.org/10.21037/ls-20-108>

Conflicts of Interest: All authors have completed the ICMJE uniform disclosure form (available at <http://dx.doi.org/10.21037/ls-20-108>). The series “Clinical Applications of Fluorescence Imaging in Laparoscopic Surgery” was commissioned by the editorial office without any funding or sponsorship. The authors have no other conflicts of interest to declare.

Ethical Statement: The authors are accountable for all aspects of the work in ensuring that questions related

to the accuracy or integrity of any part of the work are appropriately investigated and resolved.

Open Access Statement: This is an Open Access article distributed in accordance with the Creative Commons Attribution-NonCommercial-NoDerivs 4.0 International License (CC BY-NC-ND 4.0), which permits the non-commercial replication and distribution of the article with the strict proviso that no changes or edits are made and the original work is properly cited (including links to both the formal publication through the relevant DOI and the license). See: <https://creativecommons.org/licenses/by-nc-nd/4.0/>.

References

1. Bray F, Ferlay J, Soerjomataram I, et al. Global cancer statistics 2018: GLOBOCAN estimates of incidence and mortality worldwide for 36 cancers in 185 countries. *CA Cancer J Clin* 2018;68:394-424.
2. Engstrand J, Nilsson H, Stromberg C, et al. Colorectal cancer liver metastases - a population-based study on incidence, management and survival. *BMC Cancer* 2018;18:78.
3. Engstrand J, Stromberg C, Nilsson H, et al. Synchronous and metachronous liver metastases in patients with colorectal cancer-towards a clinically relevant definition. *World J Surg Oncol* 2019;17:228.
4. Shah AJ, Callaway M, Thomas MG, et al. Contrast-enhanced intraoperative ultrasound improves detection of liver metastases during surgery for primary colorectal cancer. *HPB (Oxford)* 2010;12:181-7.
5. Numata K, Morimoto M, Ogura T, et al. Ablation therapy guided by contrast-enhanced sonography with Sonazoid for hepatocellular carcinoma lesions not detected by conventional sonography. *J Ultrasound Med* 2008; 27:395-406.
6. Jones AD, Wilton JC. Can intra-operative fluorescence play a significant role in hepatobiliary surgery? *Eur J Surg Oncol* 2017;43:1622-7.
7. Kokudo N, Takemura N, Ito K, et al. The history of liver surgery: achievements over the past 50 years. *Ann Gastroenterol Surg* 2020;4:109-17.
8. Nywening TM, Tohme S, Geller DA. Laparoscopic & robotic liver resection for colorectal cancer metastases. *Laparosc Surg* 2020;4:6.
9. Beard RE, Khan S, Troisi RI, et al. Long-term and oncologic outcomes of robotic versus laparoscopic liver resection for metastatic colorectal cancer: a multicenter,

- propensity score matching analysis. *World J Surg* 2020;44:887-95.
10. Tsung A, Geller DA, Sukato DC, et al. Robotic versus laparoscopic hepatectomy: a matched comparison. *Ann Surg* 2014;259:549-55.
 11. Machi J, Sigel B. Operative ultrasound in general surgery. *Am J Surg* 1996;172:15-20.
 12. Olsen AK. Intraoperative ultrasonography and the detection of liver metastases in patients with colorectal cancer. *Br J Surg* 1990;77:998-9.
 13. Hata S, Imamura H, Aoki T, et al. Value of visual inspection, bimanual palpation, and intraoperative ultrasonography during hepatic resection for liver metastases of colorectal carcinoma. *World J Surg* 2011;35:2779-87.
 14. Handgraaf HJM, Boogerd LSF, Hoppener DJ, et al. Long-term follow-up after near-infrared fluorescence-guided resection of colorectal liver metastases: a retrospective multicenter analysis. *Eur J Surg Oncol* 2017;43:1463-71.
 15. Zhang RR, Schroeder AB, Grudzinski JJ, et al. Beyond the margins: real-time detection of cancer using targeted fluorophores. *Nat Rev Clin Oncol* 2017;14:347-64.
 16. Vahrmeijer AL, Hutteman M, van der Vorst JR, et al. Image-guided cancer surgery using near-infrared fluorescence. *Nat Rev Clin Oncol* 2013;10:507-18.
 17. Desmettre T, Devoisselle JM, Mordon S. Fluorescence properties and metabolic features of indocyanine green (ICG) as related to angiography. *Surv Ophthalmol* 2000;45:15-27.
 18. Heller MJ, Jablonski EJ. Fluorescent stokes shift probes for polynucleotide hybridization. Washington DC: U.S. Patent 4,996,143. 1991-2-26.
 19. Keereweer S, Van Driel PB, Snoeks TJ, et al. Optical image-guided cancer surgery: challenges and limitations. *Clin Cancer Res* 2013;19:3745-54.
 20. Reinhart MB, Huntington CR, Blair LJ, et al. Indocyanine green: historical context, current applications, and future considerations. *Surg Innov* 2016;23:166-75.
 21. Mordon S, Devoisselle JM, Soulie-Begu S, et al. Indocyanine green: physicochemical factors affecting its fluorescence in vivo. *Microvasc Res* 1998;55:146-52.
 22. Landsman ML, Kwant G, Mook GA, et al. Light-absorbing properties, stability, and spectral stabilization of indocyanine green. *J Appl Physiol* 1976;40:575-83.
 23. Schneider PD. Preoperative assessment of liver function. *Surg Clin North Am* 2004;84:355-73.
 24. Gotoh K, Yamada T, Ishikawa O, et al. A novel image-guided surgery of hepatocellular carcinoma by indocyanine green fluorescence imaging navigation. *J Surg Oncol* 2009;100:75-9.
 25. van der Vorst JR, Schaafsma BE, Hutteman M, et al. Near-infrared fluorescence-guided resection of colorectal liver metastases. *Cancer* 2013;119:3411-8.
 26. Kudo H, Ishizawa T, Tani K, et al. Visualization of subcapsular hepatic malignancy by indocyanine-green fluorescence imaging during laparoscopic hepatectomy. *Surg Endosc* 2014;28:2504-8.
 27. Boogerd LSF, Hoogstins CES, Schaap DP, et al. Safety and effectiveness of SGM-101, a fluorescent antibody targeting carcinoembryonic antigen, for intraoperative detection of colorectal cancer: a dose-escalation pilot study. *Lancet Gastroenterol Hepatol* 2018;3:181-91.
 28. Gutowski M, Framery B, Boonstra M, et al. SGM-101: An innovative near-infrared dye-antibody conjugate that targets CEA for fluorescence-guided surgery. *Surg Oncol* 2017;26:153-62.
 29. Keller DS, Ishizawa T, Cohen R, et al. Indocyanine green fluorescence imaging in colorectal surgery: overview, applications, and future directions. *Lancet Gastroenterol Hepatol* 2017;2:757-66.
 30. Liberale G, Bourgeois P, Larsimont D, et al. Indocyanine green fluorescence-guided surgery after IV injection in metastatic colorectal cancer: a systematic review. *Eur J Surg Oncol* 2017;43:1656-67.
 31. Alfano MS, Molfino S, Benedicenti S, et al. Intraoperative ICG-based imaging of liver neoplasms: a simple yet powerful tool. Preliminary results. *Surg Endosc* 2019;33:126-34.
 32. Van Cutsem E, Nordlinger B, Adam R, et al. Towards a pan-European consensus on the treatment of patients with colorectal liver metastases. *Eur J Cancer* 2006;42:2212-21.
 33. Takamoto T, Hashimoto T, Ichida A, et al. Surgical strategy based on indocyanine green test for chemotherapy-associated liver injury and long-term outcome in colorectal liver metastases. *J Gastrointest Surg* 2018;22:1077-88.
 34. Krieger PM, Tamandl D, Herberger B, et al. Evaluation of chemotherapy-associated liver injury in patients with colorectal cancer liver metastases using indocyanine green clearance testing. *Ann Surg Oncol* 2011;18:1644-50.
 35. Ishizawa T, Fukushima N, Shibahara J, et al. Real-time identification of liver cancers by using indocyanine green fluorescent imaging. *Cancer* 2009;115:2491-504.
 36. Uchiyama K, Ueno M, Ozawa S, et al. Combined use of contrast-enhanced intraoperative ultrasonography and a fluorescence navigation system for identifying hepatic

- metastases. *World J Surg* 2010;34:2953-9.
37. Peloso A, Franchi E, Canepa MC, et al. Combined use of intraoperative ultrasound and indocyanine green fluorescence imaging to detect liver metastases from colorectal cancer. *HPB (Oxford)* 2013;15:928-34.
 38. Kaibori M, Matsui K, Ishizaki M, et al. Intraoperative detection of superficial liver tumors by fluorescence imaging using indocyanine green and 5-aminolevulinic acid. *Anticancer Res* 2016;36:1841-9.
 39. Abo T, Nanashima A, Tobinaga S, et al. Usefulness of intraoperative diagnosis of hepatic tumors located at the liver surface and hepatic segmental visualization using indocyanine green-photodynamic eye imaging. *Eur J Surg Oncol* 2015;41:257-64.
 40. Boogerd LS, Handgraaf HJ, Lam HD, et al. Laparoscopic detection and resection of occult liver tumors of multiple cancer types using real-time near-infrared fluorescence guidance. *Surg Endosc* 2017;31:952-61.
 41. Terasawa M, Ishizawa T, Mise Y, et al. Applications of fusion-fluorescence imaging using indocyanine green in laparoscopic hepatectomy. *Surg Endosc* 2017;31:5111-8.
 42. Lieto E, Galizia G, Cardella F, et al. Indocyanine green fluorescence imaging-guided surgery in primary and metastatic liver tumors. *Surg Innov* 2018;25:62-8.
 43. Gonzalez-Ciccarelli LF, Quadri P, Daskalaki D, et al. Robotic approach to hepatobiliary surgery. *Chirurg* 2017;88:19-28.
 44. Nakaseko Y, Ishizawa T, Saiura A. Fluorescence-guided surgery for liver tumors. *J Surg Oncol* 2018;118:324-31.
 45. Peyrat P, Blanc E, Guillermet S, et al. HEPATOFLUO: A prospective monocentric study assessing the benefits of indocyanine green (ICG) fluorescence for hepatic surgery. *J Surg Oncol* 2018;117:922-7.
 46. Fretland ÅA, Dagenborg VJ, Bjørnelv GMW, et al. Laparoscopic versus open resection for colorectal liver metastases: the OSLO-COMET randomized controlled trial. *Ann Surg* 2018;267:199-207.
 47. Hamady ZZ, Lodge JP, Welsh FK, et al. One-millimeter cancer-free margin is curative for colorectal liver metastases: a propensity score case-match approach. *Ann Surg* 2014;259:543-8.
 48. Benedetti Cacciaguerra A, Görgec B, Cipriani F, et al. Risk factors of positive resection margin in laparoscopic and open liver surgery for colorectal liver metastases: a new perspective in the perioperative assessment: a European multicenter study. *Ann Surg* 2020. [Epub ahead of print]. doi: 10.1097/SLA.0000000000004077.
 49. Aoki T, Murakami M, Koizumi T, et al. Determination of the surgical margin in laparoscopic liver resections using infrared indocyanine green fluorescence. *Langenbecks Arch Surg* 2018;403:671-80.
 50. Ishizawa T, Bandai Y, Ijichi M, et al. Fluorescent cholangiography illuminating the biliary tree during laparoscopic cholecystectomy. *Br J Surg* 2010;97:1369-77.
 51. Ishizawa T, Tamura S, Masuda K, et al. Intraoperative fluorescent cholangiography using indocyanine green: a biliary road map for safe surgery. *J Am Coll Surg* 2009;208:e1-4.
 52. Ankersmit M, van Dam DA, van Rijswijk AS, et al. Fluorescent imaging with indocyanine green during laparoscopic cholecystectomy in patients at increased risk of bile duct injury. *Surg Innov* 2017;24:245-52.
 53. Dip F, LoMenzo E, Sarotto L, et al. Randomized trial of near-infrared incisionless fluorescent cholangiography. *Ann Surg* 2019;270:992-9.
 54. Kobayashi Y, Kawaguchi Y, Kobayashi K, et al. Portal vein territory identification using indocyanine green fluorescence imaging: technical details and short-term outcomes. *J Surg Oncol* 2017;116:921-31.
 55. Ueno M, Hayami S, Sonomura T, et al. Indocyanine green fluorescence imaging techniques and interventional radiology during laparoscopic anatomical liver resection (with video). *Surg Endosc* 2018;32:1051-5.
 56. Nishino H, Hatano E, Seo S, et al. Real-time navigation for liver surgery using projection mapping with indocyanine green fluorescence: development of the novel medical imaging projection system. *Ann Surg* 2018;267:1134-40.
 57. van Keulen S, Nishio N, Birkeland A, et al. The sentinel margin: intraoperative ex vivo specimen mapping using relative fluorescence intensity. *Clin Cancer Res* 2019;25:4656-62.
 58. Tiernan JP, Perry SL, Verghese ET, et al. Carcinoembryonic antigen is the preferred biomarker for in vivo colorectal cancer targeting. *Br J Cancer* 2013;108:662-7.
 59. Hoogstins CES, Boogerd LSF, Sibinga Mulder BG, et al. Image-guided surgery in patients with pancreatic cancer: first results of a clinical trial using SGM-101, a novel carcinoembryonic antigen-targeting, near-infrared fluorescent agent. *Ann Surg Oncol* 2018;25:3350-7.
 60. Schaap DP, de Valk KS, Deken MM, et al. Carcinoembryonic antigen-specific, fluorescent image-guided cytoreductive surgery with hyperthermic intraperitoneal chemotherapy for metastatic colorectal cancer. *Br J Surg* 2020;107:334-7.

61. Meijer RPJ, de Valk KS, Deken MM, et al. Intraoperative detection of colorectal and pancreatic liver metastases using SGM-101, a fluorescent antibody targeting CEA. *Eur J Surg Oncol* 2021;47:667-73.
62. Lim YT, Kim S, Nakayama A, et al. Selection of quantum dot wavelengths for biomedical assays and imaging. *Mol Imaging* 2003;2:50-64.
63. Hu Z, Fang C, Li B, et al. First-in-human liver-tumour surgery guided by multispectral fluorescence imaging in the visible and near-infrared-I/II windows. *Nat Biomed Eng* 2020;4:259-71.
64. Cao J, Zhu B, Zheng K, et al. Recent progress in NIR-II contrast agent for biological imaging. *Front Bioeng Biotechnol* 2020;7:487.
65. Yu H, Ji M. Recent advances of organic near-infrared II fluorophores in optical properties and imaging functions. *Mol Imaging Biol* 2021;23:160-72.
66. Lakowicz JR. Quenching of fluorescence. In: Lakowicz JR. editor. *Principles of fluorescence spectroscopy*. Boston: Springer, 2006:277-330.
67. Wang S, Fan Y, Li D, et al. Anti-quenching NIR-II molecular fluorophores for in vivo high-contrast imaging and pH sensing. *Nat Commun* 2019;10:1058.

doi: 10.21037/ls-20-108

Cite this article as: Bijlstra OD, Achterberg FB, Grosheide L, Vahrmeijer AL, Swijnenburg RJ. Fluorescence-guided minimally-invasive surgery for colorectal liver metastases, a systematic review. *Laparosc Surg* 2021;5:32.